



## A new nonreflecting open boundary condition for circular cavities in unbounded domain

Mohsen Mirzajani and Naser Khaji

Faculty of Civil and Environmental Engineering, Tarbiat Modares University, P.O. Box 14115–397,  
Tehran, Iran.

nkhaji@modares.ac.ir

### Abstract

In this paper, a new non-reflecting open boundary condition is introduced in order to solve circular cavity problems. In this regard, a new semi-analytical method is used to diagonalize the coefficient matrices of governing differential equation. This method uses four tools in order to diagonalize the coefficient matrices in which they are: higher-order sub-parametric elements, higher-order Chebyshev mapping functions, weighted residual method and Clenshaw-Curtis quadrature. This method is developed to diagonalize the dynamic stiffness matrix. To this aim, the substructure method is used. Two first order ordinary differential equations (i.e. interaction force-displacement relationship and governing differential equation in dynamic stiffness) are solved to satisfy the radiation condition at infinity and boundary condition of soil-structure interface. The interaction force-displacement relationship is considered as a nonreflecting open boundary condition for the bounded medium substructure. Two cavities embedded in a full-plane are considered as benchmark examples and the results are compared with analytical solutions.

**Keywords:** semi-analytical method, open nonreflecting boundary condition, Chebyshev polynomial, sub-parametric elements.

### 1. INTRODUCTION

The dynamic analysis of medium-structure interaction based on substructure method requires investigating the dynamic response of unbounded media. In this regard, the dynamic stiffness matrix should be determined in the frequency domain. The dynamic property of unbounded domain could be illustrated by force-displacement relationship formulated at the medium-structure interface. In the substructure method, this relationship could be regarded as a Boundary Condition (BC) for bounded substructure.

Excellent literature reviews about open BCs are discussed in [1-4]. The higher order open boundaries increase the accuracy as their order of approximation increases [5]. Also, the formulations of these BCs are temporally local and are singly asymptotic at the high frequency limit. The doubly asymptotic boundaries are introduced to model an unbounded domain with the presence of nonradiative wave fields [6-9]. Various local BCs have been proposed [10-11]. These BCs are simple, approximate and should be generally applied to a boundary sufficiently far from the region of interest.

In the frequency domain analysis, the dynamic stiffness matrix of the unbounded medium is required to be determined. The soil stiffness matrix may be derived by implementing FEM [12], BEM [13], SEM [14] and SBFEM [15].

The goal of this paper is to introduce a new semi-analytical method for diagonalization of dynamic stiffness matrix and proposing a new non-reflecting BC for circular cavity problems. The present method has been recently developed for solving potential [16], elastostatic [17, 18] and elastodynamic problems in the time [19] and the frequency [20] domains. In this method, only the boundaries of the problem's domain are discretized with higher-order sub-parametric elements. Using the weighted residual method and implementing Clenshaw-Curtis quadrature leads to a diagonal system of Bessel's differential equation, in the frequency domain. In other words, the governing differential equation for each DOF is independent from other DOFs. In this method, the far field radiation BC at infinity is satisfied, exactly.

### 2. SUMMARY OF NEW SEMI-ANALYTICAL METHOD

In order to explain the principals of the new semi-analytical method, an unbounded domain as shown in figure 1 in considered.

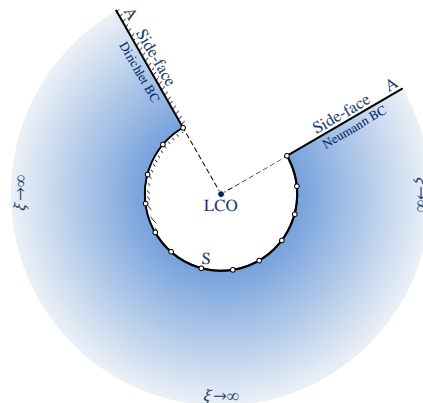


**Figure 1. Soil-structure interface of unbounded medium with Dirichlet and Neumann BCs without spatial discretization**

In this method the LCO is selected at a point from which the whole problem's domain is visible. After choosing the LCO, the structure-medium interface is discretized implementing new sub-parametric elements. In this method higher-order Chebyshev polynomials is used as mapping functions. In the local coordinate, using  $n_\eta + 1$  mapping functions of  $\varphi_i(\eta)$  are as follow

$$x(\eta) = \sum_{i=1}^{n_\eta+1} \varphi_i(\eta) x_i, \quad y(\eta) = \sum_{i=1}^{n_\eta+1} \varphi_i(\eta) y_i. \quad (1)$$

Also, any given point in the domain may be computed using following expression

$$\hat{x}(\xi, \eta) = \xi x(\eta), \quad \hat{y}(\xi, \eta) = \xi y(\eta). \quad (2)$$

In order to transform the global coordinates into local coordinates the Jacobian matrix is used as follow

$$\hat{\mathbf{J}}(\xi, \eta) = \begin{bmatrix} \hat{x}_{,\xi}(\xi, \eta) & \hat{y}_{,\xi}(\xi, \eta) \\ \hat{x}_{,\eta}(\xi, \eta) & \hat{y}_{,\eta}(\xi, \eta) \end{bmatrix}. \quad (3)$$

The relation between a differential element of area in the global coordinates and a differential element of area in the local coordinates may be written as follow

$$d\Omega = d\hat{x} d\hat{y} = |\hat{\mathbf{J}}(\xi, \eta)| d\xi d\eta = \xi |\mathbf{J}(\eta)| d\xi d\eta. \quad (4)$$

In the following, the anti-plane motion is considered. The displacement field is scalar. The spatial derivatives for two coordinate systems are considered as follow

$$\begin{Bmatrix} \frac{\partial}{\partial \hat{x}} \\ \frac{\partial}{\partial \hat{y}} \end{Bmatrix} = \mathbf{b}_A^1(\eta) \frac{\partial}{\partial \xi} + \mathbf{b}_A^2(\eta) \frac{1}{\xi} \frac{\partial}{\partial \eta}, \quad (5)$$

Where

$$\mathbf{b}_A^1(\eta) = \frac{1}{|\mathbf{J}|} \begin{Bmatrix} y_{,\eta}(\eta) \\ -x_{,\eta}(\eta) \end{Bmatrix}, \quad \mathbf{B}_A^1(\eta) = \mathbf{b}_A^1 \mathbf{N}, \quad (6)$$

$$\mathbf{b}_A^2(\eta) = \frac{1}{|\mathbf{J}|} \begin{Bmatrix} -y(\eta) \\ x(\eta) \end{Bmatrix}, \quad \mathbf{B}_A^2(\eta) = \mathbf{b}_A^2 \mathbf{N}. \quad (7)$$

The strain vector may be obtained as follow



$$\hat{\boldsymbol{\varepsilon}}(\zeta, \eta, \omega) = \left[ \hat{\boldsymbol{\varepsilon}}_x(\zeta, \eta, \omega) \quad \hat{\boldsymbol{\varepsilon}}_y(\zeta, \eta, \omega) \right]^T = \mathbf{b}_A^1(\eta) \mathbf{N} \hat{\mathbf{u}}_{z,\zeta} + \frac{1}{\zeta} \mathbf{b}_A^2(\eta) \mathbf{N}_\eta \hat{\mathbf{u}}_z. \quad (8)$$

Moreover, the stress-strain relationship may be written as

$$\hat{\boldsymbol{\sigma}}(\zeta, \eta, \omega) = G \hat{\boldsymbol{\varepsilon}}(\zeta, \eta, \omega), \quad (9)$$

where  $G$  is the shear modulus of the problem's medium. For the anti-plane motion, the governing equation in the frequency domain may be written as follow

$$\hat{\sigma}_{z_{ij},j} + \hat{f}_{zi} + \rho \omega^2 \hat{u}_{zi} = 0. \quad (10)$$

where  $\hat{\sigma}_{z_{ij}}$  denotes the stress tensor components,  $\hat{f}_{zi}$  refers to the external source of exciting forces generated per unit volume for anti-plane motion. After some mathematical manipulation the governing differential equation may be derived as [20]

$$\zeta \mathbf{D}_A^0 \hat{\mathbf{u}}_{z,\zeta\zeta} + \mathbf{D}_A^1 \hat{\mathbf{u}}_{z,\zeta} + \omega^2 \zeta \mathbf{M}_A \hat{\mathbf{u}}_z + \zeta \hat{\mathbf{F}}_A^b(\zeta, \omega) = \mathbf{0}, \quad (11)$$

in which

$$\mathbf{D}_A^0 = G \int_{-1}^{+1} \mathbf{B}_A^T \mathbf{B}_A |\mathbf{J}| d\eta, \quad (12)$$

$$\mathbf{D}_A^1 = G \int_{-1}^{+1} \mathbf{B}_{A,\eta}^T \mathbf{B}_A^2 |\mathbf{J}| d\eta, \quad (13)$$

$$\mathbf{M}_A = \rho \int_{-1}^{+1} \mathbf{N}^T \mathbf{N} |\mathbf{J}| d\eta, \quad (14)$$

$$\hat{\mathbf{F}}_A^b = \int_{-1}^{+1} \mathbf{N}^T \hat{\mathbf{f}}_A^b |\mathbf{J}| d\eta. \quad (15)$$

The present new semi-analytical method employs four special tools in order to diagonalize the coefficient matrices [20]. For the anti-plane motion, the coefficient matrices may be written in diagonalized form as follow

$$D_{Aij}^0 = 2\delta_{ij} W_i \mathbf{B}_A^{1T}(\eta_i) G \mathbf{B}_A^1(\eta_i) |\mathbf{J}(\eta_i)|, \quad (16)$$

$$D_{Aij}^1 = 2\delta_{ij} W_i \mathbf{B}_{A,\eta}^{1T}(\eta_i) G \mathbf{B}_A^2(\eta_i) |\mathbf{J}(\eta_i)|, \quad (17)$$

$$M_{Aij} = 2\delta_{ij} W_i \mathbf{N}^T(\eta_i) \rho \mathbf{N}(\eta_i) |\mathbf{J}(\eta_i)|, \quad (18)$$

values of Clenshaw–Curtis quadrature. After diagonalization of coefficient matrices, the diagonal set of Bessel's differential equations for  $i$ th DOF, as given by the following relation

$$\zeta D_{Aii}^0 \hat{u}_{z_i,\zeta\zeta} + D_{Aii}^1 \hat{u}_{z_i,\zeta} + \omega^2 \zeta M_{Aii} \hat{u}_{z_i} + \zeta \hat{F}_{Aci}^b = 0. \quad (19)$$

### 3. A NEW NONREFLECTING OPEN BOUNDARY CONDITION

In the present new semi-analytical method the substructure method is used. The dynamic behavior of unbounded medium is described by the interaction force-displacement relationship on the medium-structure interface. The interaction force-displacement relationship could be regarded as a global open BC. . In the present method, the LCO is identical for all nodes. In other words, the LCO has the same displacement components for all nodes. Therefore, the physical concept of this phenomenon may be considered as a few parallel springs with distinct stiffnesses, which adjoin to each other at the LCO.

In the frequency domain, the relation between displacement vector and interaction forces vector could be expressed using the dynamic-stiffness matrix as follow

$$\mathbf{R}(\omega) = \mathbf{S}^\infty(\omega) \hat{\mathbf{u}}(\omega). \quad (20)$$



Eq. (20) could be considered as a global open BC at the present method. As linear behavior of the domain is considered in the present paper, the Fourier and Inverse Fourier transformation may be applied. Applying the Inverse Fourier transformation to Eq. (20) yields

$$\mathbf{R}(t) = \int_0^t \mathbf{S}^\infty(t - \tau) \mathbf{u}(\tau) d\tau . \quad (21)$$

which is a convolution integral that is diagonalized using the present method. In other word, each DOF is independent from other DOFs. In order to compute the interaction force-displacement relationship, the internal nodal forces  $\mathbf{Q} = \mathbf{Q}(\xi)$  plus the redistribution effect, for internal nodal forces appeared in the present method are considered. The principle of virtual work yields

$$\mathbf{w}^T \mathbf{Q} = \int_{S^\xi} w \mathbf{n}^{\xi T} \boldsymbol{\sigma} dS^\xi , \quad (22)$$

in which  $dS^\xi$  and  $w$  are determined as (see Figure 2).

$$dS^\xi = \sqrt{\hat{x}_{,\eta}^2(\eta) + \hat{y}_{,\eta}^2(\eta)} d\eta = \xi \sqrt{x_{,\eta}^2(\eta) + y_{,\eta}^2(\eta)} d\eta , \quad (23)$$

$$w = w(\xi, \eta, \omega) = \mathbf{N}(\eta) \mathbf{w}(\xi, \omega) . \quad (24)$$

For an arbitrary  $\mathbf{w}(\xi, \omega)$  one may write

$$\mathbf{Q} = \xi \int_{-1}^{+1} \mathbf{N}^T \mathbf{b}^{1T} \boldsymbol{\sigma} |\mathbf{J}| d\eta . \quad (25)$$

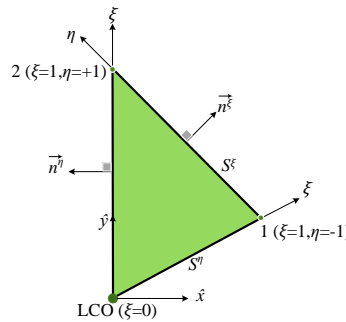


Figure 2. Schematic view of a sample 2D domain, in which the LCO is shown in local coordinate systems

By substituting Eqs. (6) and (9) into Eq. (25) and considering the redistribution effects of the present method, one may write

$$\mathbf{Q} = \xi \int_{-1}^{+1} \mathbf{B}^{1T} \mathbf{G} \mathbf{B}^1 \hat{\mathbf{u}}_{A,\xi} |\mathbf{J}| d\eta + \varsigma \int_{-1}^{+1} \mathbf{B}^{1T} \mathbf{G} \mathbf{B}^1 \hat{\mathbf{u}}_A |\mathbf{J}| d\eta , \quad (26)$$

or

$$\mathbf{Q}_A = \xi \mathbf{D}_A^0 \hat{\mathbf{u}}_{A,\xi} + \varsigma \mathbf{D}_A^0 \hat{\mathbf{u}}_A , \quad (27)$$

in which the redistribution coefficients are introduced as follow

$$\varsigma_{Aii} = \frac{D_{Aii}^0 - \chi_{Ai} D_{Aii}^1}{\sum_{j=1}^m D_{Ajj}^0} , \quad \chi_{Aii} = \frac{D_{Aii}^1}{\sum_{j=1}^m D_{Ajj}^1} \quad (28)$$

Implementing the new semi-analytical method, Eq. (27) may be written in decoupled form as follow

$$\begin{Bmatrix} Q_{1z} \\ \vdots \\ Q_{nz} \end{Bmatrix}_A = \xi \begin{bmatrix} D_{11z}^0 & \cdots & 0 \\ \vdots & \ddots & \vdots \\ 0 & \cdots & D_{mz}^0 \end{bmatrix}_A \begin{Bmatrix} \hat{u}_{1z} \\ \vdots \\ \hat{u}_{nz} \end{Bmatrix}_{A,\xi} + \varsigma_{Aii} \begin{bmatrix} D_{11z}^0 & \cdots & 0 \\ \vdots & \ddots & \vdots \\ 0 & \cdots & D_{mz}^0 \end{bmatrix}_A \begin{Bmatrix} \hat{u}_{1z} \\ \vdots \\ \hat{u}_{nz} \end{Bmatrix}_A , \quad (29)$$

or

$$Q_{Ai} = \xi D_{Aii}^0 \hat{u}_{A,i,\xi} + \varsigma_{Aii} D_{Aii}^0 \hat{u}_{Ai} . \quad (30)$$



The internal nodal force vector  $\mathbf{Q}(\xi)$  and nodal forces' vector  $\mathbf{R}(\xi)$  may be related with each other as

$$\mathbf{R} = \pm \mathbf{Q}, \quad (31)$$

in which positive and negative signs represent the bounded and unbounded media, respectively. Eq. (20) may be written as follow

$$\mathbf{R}(\xi) = \mathbf{S}(\xi, \omega) \hat{\mathbf{u}}(\xi) - \mathbf{R}^F(\xi), \quad (32)$$

where  $\mathbf{R}^F(\xi)$  implies the amplitude of nodal force due to the body load and surface traction. substituting Eq. (27) and (32) into Eq. (33) yields

$$\pm \mathbf{S} \hat{\mathbf{u}}_A \mp \mathbf{R}^F = \zeta \mathbf{D}_A^0 \hat{\mathbf{u}}_{A,\zeta} + \varsigma \mathbf{D}_A^0 \hat{\mathbf{u}}_A, \quad (33)$$

After differentiating and some mathematical manipulation the governing differential equations in dynamic-stiffness in the frequency domain for unbounded media may be written as follow

$$-\omega \mathbf{S}_{,\omega}^\infty + \mathbf{D}_A^{0-1} \mathbf{S}^{\infty 2} - (\chi_A \mathbf{D}_A^{0-1} \mathbf{D}_A^1 - 2\zeta) \mathbf{S}^\infty + \varsigma (-\chi_A \mathbf{D}_A^1 + \zeta \mathbf{D}_A^0) - n^2 \mathbf{D}_A^0 + \omega^2 \zeta^2 \mathbf{M}_A = \mathbf{0}, \quad (34)$$

This equation is the system of non-linear first-order ordinary differential equations with the frequency  $\omega$ , which is diagonalized with the new semi-analytical method. The decoupled form of EQ. (35) may be written as follow

$$-\omega S_{ii,\omega}^\infty + \frac{1}{D_{Aii}^0} S_{ii}^{\infty 2} - (\chi_{Aii} \frac{D_{Aii}^1}{D_{Aii}^0} - 2\zeta_{Aii}) S_{ii}^\infty + \varsigma_{Aii} (-\chi_{Aii} D_{Aii}^1 + \zeta_{Aii} D_{Aii}^0) - n^2 D_{Aii}^0 + \omega^2 \zeta^2 M_{Aii} = 0, \quad (35)$$

In static status, the governing differential equations in displacement and stiffness may be yield to diagonal coefficient of static-stiffness matrix of unbounded domain as

$$K_{ii}^\infty = \frac{1}{2} \left( \chi_{Aii} D_{Aii}^1 - 2\zeta_{Aii} D_{Aii}^0 + \sqrt{4n^2 D_{Aii}^0{}^2 + \chi_{Aii}^2 D_{Aii}^1{}^2} \right). \quad (36)$$

### 3.1. ASYMPTOTIC EXPANSION FOR HIGH FREQUENCY

To this aim, the governing differential equation in dynamic stiffness should be solved starting at a high but finite frequency ( $\omega_h$ ) from high frequency asymptotic expansion. In this regard, the dynamic-stiffness matrix is extended in a power series of order  $m$  as follow

$$\mathbf{S}^\infty(\omega) \approx i\omega \mathbf{C}_\infty + \mathbf{K}_\infty + \sum_{j=1}^m \frac{1}{(i\omega)^j} \mathbf{A}_j, \quad (37)$$

The first two terms on the right hand side of Eq. (38) shows the singular part  $\mathbf{S}_s^\infty(\omega)$  with the constant dashpot matrix  $\mathbf{C}_\infty$  and the constant spring matrix  $\mathbf{K}_\infty$ . The third term indicates the regular part  $\mathbf{S}_r^\infty(\omega)$ , which is expanded implementing  $m$  terms of the power series with the unknown coefficient matrices  $\mathbf{A}_j$ .

The eigenvalue problem is considered as

$$\mathbf{M}\Phi = \mathbf{D}^0 \Phi \Lambda^2, \quad (38)$$

the eigenvectors  $\Phi$  are normalized as given by

$$\Phi^T \mathbf{D}^0 \Phi = \mathbf{I}, \quad (39)$$

In addition

$$\Phi^T \mathbf{M}\Phi = \Lambda^2, \quad (40)$$

$$\mathbf{D}^{0-1} = \Phi \Phi^T, \quad (41)$$

Introducing the normalize form of matrices as

$$\mathbf{s}^\infty = \Phi^T \mathbf{S}^\infty \Phi, \quad (42)$$

$$\mathbf{c}_\infty = \Phi^T \mathbf{C}_\infty \Phi, \quad (43)$$

$$\mathbf{k}_\infty = \Phi^T \mathbf{K}_\infty \Phi, \quad (44)$$



$$\mathbf{a}_j = \mathbf{\Phi}^T \mathbf{A}_j \mathbf{\Phi}, \quad (45)$$

and considering  $m=2$  one may write

$$\mathbf{c}_\infty = \mathbf{\Lambda}, \quad \mathbf{C}_\infty = \mathbf{\Phi}^{-T} \mathbf{\Lambda} \mathbf{\Phi}^{-1}. \quad (46)$$

$$\mathbf{k}_\infty = \frac{1}{2} \left( (-2\zeta + \chi \mathbf{e}^1) + \mathbf{I} \right), \quad \mathbf{K}_\infty = \mathbf{\Phi}^{-T} \mathbf{k}_\infty \mathbf{\Phi}^{-1}. \quad (47)$$

$$\mathbf{a}_1 = \frac{1}{2} \mathbf{\Lambda}^{-1} \left( n^2 \mathbf{I} - \mathbf{k}_\infty^2 + (-2\zeta + \chi \mathbf{e}^1) \mathbf{k}_\infty - \zeta (-\chi \mathbf{e}^1 + \zeta) \right), \quad (48)$$

$$\mathbf{a}_2 = \frac{1}{2} \mathbf{\Lambda}^{-1} \left( -\mathbf{a}_1 - 2\mathbf{k}_\infty \mathbf{a}_1 + (-2\zeta + \chi \mathbf{e}^1) \mathbf{a}_1 \right), \quad \mathbf{A}_j = \mathbf{\Phi}^{-T} \mathbf{a}_j \mathbf{\Phi}^{-1} \quad (49)$$

### 3.2. UNIT-IMPULSE RESPONSE

Considering Eq. (38), the regular part of EQ. (38) is square integrable. Using the inverse Fourier transform, the unit-impulse response may be obtained from

$$\mathbf{S}_r^\infty(t) = \mathbf{C}_\infty \dot{\delta}(t) + \mathbf{K}_\infty \delta(t) + \mathbf{S}_r^\infty(t), \quad (50)$$

where  $\delta(t)$  indicates the Dirac delta function, and  $\mathbf{S}_r^\infty(\omega)$  and  $\mathbf{S}_r^\infty(t)$  are Fourier transform pairs.

Implementing inverse Fourier transform yields

$$\mathbf{R}(t) = \mathbf{C}_\infty \dot{\mathbf{u}}(t) + \mathbf{K}_\infty \mathbf{u}(t) + \int_0^t \mathbf{S}_r^\infty(t - \tau) \mathbf{u}(\tau) d\tau, \quad (51)$$

The first two terms on the right-hand side of Eq. (52) depicts the instantaneous response, and the convolution integral indicates the delaying part of the response. Using the following abbreviation

$$\mathbf{V}_r^\infty(\omega) = \frac{1}{i\omega} \mathbf{S}_r^\infty(\omega), \quad (52)$$

may yields to following relation

$$\mathbf{S}_r^\infty(t) = \mathbf{C}_\infty \dot{\delta}(t) + \mathbf{K}_\infty \delta(t) + \mathbf{A}_1 H(t), \quad (53)$$

where  $H(t)$  denotes the Heaviside step function. By comparing Eqs. (51) and (54) at  $t = 0$ , the regular part of the unit-impulse response matrix is evaluated as given by

$$\mathbf{S}_r^\infty(0) = \mathbf{A}_1, \quad (54)$$

And finally for  $t = m\Delta t$  after some mathematical manipulation one may obtained

$$\begin{aligned} & \left[ \frac{2}{\Delta t} \mathbf{D}^{0-1} \mathbf{C}_\infty + \mathbf{D}^{0-1} \mathbf{K}_\infty - \frac{1}{2} \chi \mathbf{D}^{0-1} \mathbf{D}^1 + \zeta + \left(m - \frac{1}{2}\right) \mathbf{I} \right] \mathbf{V}_{r^m}^\infty \\ & = -\mathbf{D}^{0-1} \sum_{j=1}^{m-1} \mathbf{V}_{r^j}^\infty \mathbf{V}_{r^{m-j}}^\infty - \left[ 2\mathbf{D}^{0-1} \mathbf{K}_\infty - \chi \mathbf{D}^{0-1} \mathbf{D}^1 + 2\zeta + \mathbf{I} \right] \sum_{j=1}^{m-1} \mathbf{V}_{r^j}^\infty \\ & - m \left[ \mathbf{D}^{0-1} \mathbf{K}_\infty^2 - (\chi \mathbf{D}^{0-1} \mathbf{D}^1 - 2\zeta) \mathbf{K}_\infty + \zeta (-\chi \mathbf{D}^1 + \zeta \mathbf{D}^0) - n^2 \mathbf{D}^0 \right] \end{aligned} \quad (55)$$

The regular part of the unit-impulse response matrix  $\mathbf{S}_{r^m}^\infty$  is calculated as

$$\mathbf{S}_{r^m}^\infty = \frac{1}{\Delta t} \left( \mathbf{V}_{r^m}^\infty - \mathbf{V}_{r^{m-1}}^\infty \right), \quad (56)$$

## 4. NUMERICAL EXAMPLES

In order to assess the accuracy of the proposed method, two cavity problems are considered. The results of the present method are compared with analytical solutions available in literature. No physical damping is considered. The measurements are in the SI units.

### 4.1. ANTI-PLANE MOTION OF CIRCULAR CAVITY EMBEDDED IN FULL-PLANE



The anti-plane motion of a circular cavity of radius  $r_0$  embedded in a full-plane is considered as shown in Figure 3. In this example, the propagation of each mode is one-dimensional and can be explained analytically. The Poisson's ratio of the problem's material is  $\nu = \frac{1}{3}$ . The anti-plane displacement  $\hat{u}_0(\omega)$  with exciting frequency  $\omega$  is applied to the structure-medium interface as shown in Figure 3.

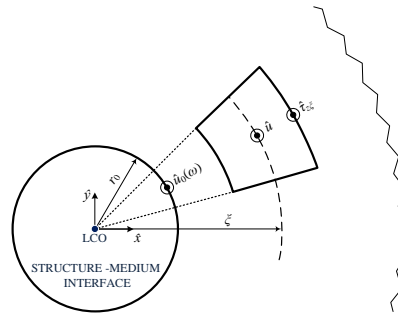


Figure 3. Anti-plane motion of circular cavity embedded in a full-plane

In this example, due to symmetry, only one-quarter of the structure-medium interface is discretized using 4 three-node elements of equal length. For the 1<sup>st</sup> DOF the redistribution coefficients are calculated as

$$\chi_{A_{11}} \approx 0.04, \quad \zeta_{A_{11}} \approx 0.02 \quad (58)$$

Then, the governing differential equation for displacement is written as

$$\xi^2 \hat{u}_{A_{3,\xi\xi}} + 1.04 \xi \hat{u}_{A_{3,\xi}} - n^2 \hat{u}_{A_3} + \left(\frac{\omega \xi}{c_s}\right)^2 \hat{u}_{A_3} = 0, \quad (59)$$

The results of the present method are compared with the exact solution for the mode numbers of  $n=0,1$  in Figures 4, 5, respectively. The unit-impulse response coefficient is calculated using the present method and compared with exact solution in Figure 6. Excellent agreement is obtained.

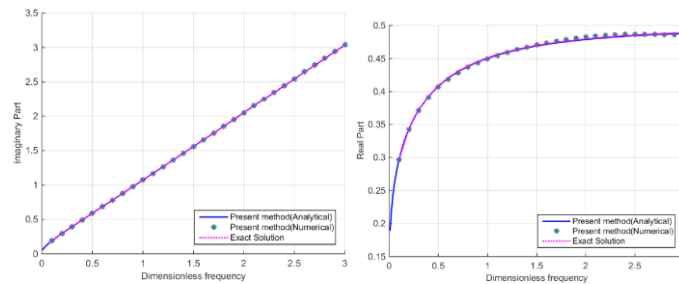


Figure 4. Dynamic stiffness coefficient of second example, for the mode number of  $n=0$

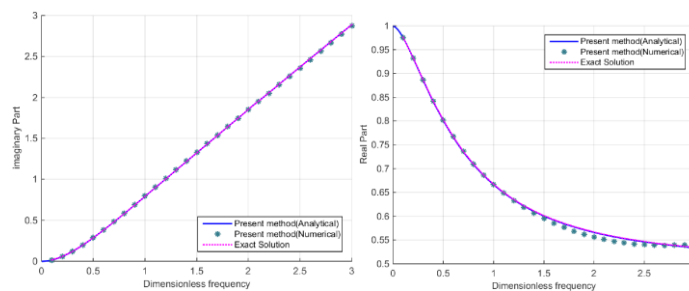


Figure 5. Dynamic stiffness coefficient of second example, for the mode number of  $n=1$

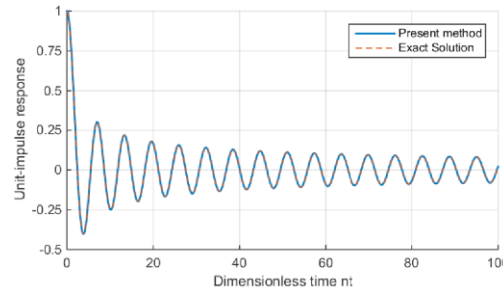


Figure 6. Unit-impulse response of circular cavity embedded in full-plane

#### 4.2. IN-PLANE MOTION OF CIRCULAR CAVITY EMBEDDED IN FULL-PLANE

A circular cavity embedded in a homogeneous full-plane as shown in Figure 7 is considered. Again, the Poisson's ratio of the problem's material is  $\nu = \frac{1}{3}$ . A translational displacement  $\hat{u}_0(\omega)$  is applied to the structure-medium interface (see Figure 7). Because of symmetry, only one-quarter of the structure-medium interface is discretized using 4 three-node elements with equal length.

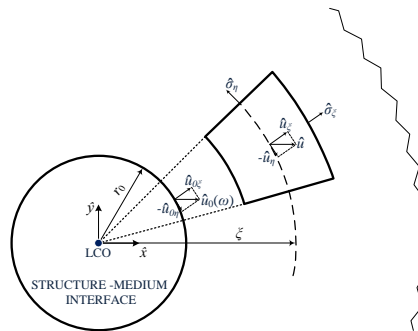


Figure 7. In-plane motion of circular cavity embedded in a full-plane

The results of the present method are compared with analytical solution in Figure 8. As may be observed from Figure 8, there are excellent agreements between the results.

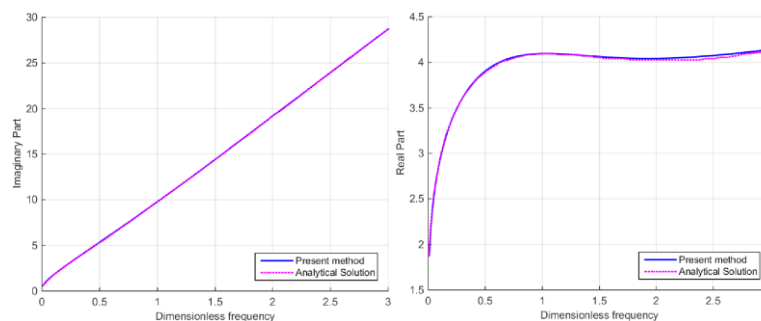


Figure 8. Dynamic-stiffness coefficient of second example

#### 5. CONCLUSION

In this paper a new semi-analytical method is developed in order to diagonalization of dynamic stiffness matrix in the frequency domain. A new global open boundary condition has been proposed for unbounded media. In this method, only the problem's domain boundary should be discretized which yields to a set of decoupled Bessel's differential equations in the frequency domain. They include interaction force-





displacement relationship and governing differential equation in dynamic stiffness has been developed using the new semi-analytical method. Two cavities embedded in a full-plane are selected as the benchmark examples. Excellent agreement is obtained.

## 11. REFERENCES

1. Givoli D. (2004) "High-order local non-reflecting boundary conditions: a review". *Wave Motion*, **39**:319–326.
2. Givoli D. (1991) "Non-reflecting boundary conditions: a review". *Journal of Computational Physics*, **94**:1–29.
3. Astley RJ. (2000) "Infinite elements for wave problems: a review of current formulations and an assessment of accuracy". *International Journal for Numerical Methods in Engineering*, **49**:951–976.
4. Kausel E. (1988) "Local transmitting boundaries". *Journal of Engineering Mechanics (ASCE)*, **114**:1011–1027.
5. S. V. Tsynkov, (1998) "Numerical solution of problems on unbounded domains. A review," *Applied Numerical Mathematics*, **27**(4): 465–532.
6. T. L. Geers, (1978) "Doubly asymptotic approximations for transient motions of submerged structures," *Journal of the Acoustical Society of America*, **64**(5), 1500–1508.
7. T. Geers, (1998) "Singly and doubly asymptotic computational boundaries," in *Proceedings of the IUTAM Symposium on Computational Methods for Unbounded Domains*, 135–141, Kluwer Academic Publishers.
8. T. L. Geers and B. A. Lewis, (1997) "Doubly asymptotic approximations for transient elastodynamics," *International Journal of Solids and Structures*, **34**(11), 1293–1305.
9. P. Underwood and T. L. Geers, (1981) "Doubly asymptotic, boundary-element analysis of dynamic soilstructure interaction," *International Journal of Solids and Structures*, **17**(7), 687–697.
10. Smith WD. (1974) "A nonreflecting plane boundary for wave propagation problems". *Journal of Computational Physics*, **15**, 492–503.
11. Liao ZP, Wong HL. (1984) "A transmitting boundary for the numerical simulation of elastic wave propagation". *International Journal of Soil Dynamics and Earthquake Engineering*, **3**, 174–183.
12. Sharma KG. (1985) "Condensation of elastic half space soil stiffness matrix considering symmetry". *International Journal for Numerical and Analytical Methods in Geomechanics*, **9**, 391–395.
13. Dominguez J. (1993) "*Boundary Elements in Dynamics*". Computational Mechanics Publications: Southampton.
14. Komatitsch D, Ritsema J, Tromp J. (2002) "The spectral-element method, Beowulf computing and global seismology". *Science*, **298**(5599):1737–1742.
15. Wolf JP. (2004) "*The Scaled Boundary Finite Element Method*". Wiley: New York.
16. Khaji N, Khodakarami MI. (2011) "A new semi-analytical method with diagonal coefficient matrices for potential problems". *Engineering Analysis with Boundary Elements*, **35**, 845–854.
17. Khodakarami MI., Khaji N. (2011) "Analysis of elastostatic problems using a semi-analytical method with diagonal coefficient matrices". *Engineering Analysis with Boundary Elements*, **35**, 1288–1296.
18. Khaji N, Khodakarami MI. (2012) "A semi-analytical method with a system of decoupled ordinary differential equations for three-dimensional elastostatic problems". *International Journal of Solids and Structures*, **49**, 2528–2546.
19. Khodakarami MI, Khaji N, Ahmadi MT. (2012) "Modeling transient elastodynamic problems using a novel semi-analytical method yielding decoupled partial differential equations". *Computer Methods in Applied Mechanics and Engineering*, **213**, 183–195.
20. Khaji N, Mirzajani M. (2013) "Frequency domain analysis of elastic bounded domains using a new semi-analytical method". *Acta Mechanica*, **224**, 1555–1570.